Rhodaoxetane: Synthesis, Structure, and Theoretical Evaluation

Maria J. Calhorda,*,† Adelino M. Galvão,‡ and Canan Ünaleroglu‡,§

Instituto de Tecnologia Química e Biológica, R. Quinta Grande 6, Apart. 127, 2780 Oeiras and Instituto Superior Técnico, Av. Rovisco Pais, 1096 Lisboa Codex, Portugal, and Centro de Química Estrutural, IST, Av. Rovisco Pais, 1096 Lisboa Codex, Portugal

Andrei A. Zlota, Felix Frolow, and David Milstein*

Department of Organic Chemistry, The Weizmann Institute of Science, Rehovot 76100, Israel

Received April 9, 1993

Oxidative addition of $Rh(PMe_3)_3Cl$ to $HOCMe_2CH_2Br$ leads to the β-hydroxy complex **4**. Deprotonation of **4** with $(Me_3Si)_2NK$ leads to the rhodaoxetane **5**. **4** and **5** were crystallographically characterized, allowing direct evaluation of the structural consequences of ring closure. The oxetane ring in **5** is planar and it exhibits Rh–C [2.069(10) Å] and C–O [1.416(12) Å], significantly shorter than the equivalent bonds in **4**. The planarity of the oxetane ring was assigned to a minimization of repulsive interactions between filled orbitals of the metal and oxygen in this geometry, a result of a theoretical study based on extended Hückel calculations. **4** also shows a substantial Cl···H hydrogen bond. **5** can also be obtained by direct oxidative addition of $Rh(PMe_3)_3Br$ to isobutylene oxide, providing the first direct demonstration of oxidative addition of a metal complex to a simple epoxide to yield a metallaoxetane. Calculations were done in order to probe the reactivity of the metallacycle.

Introduction

The intermediacy of 2-metallaoxetanes has been proposed in various important processes, such as metal catalyzed oxidations,[1] although their possible involvement in cytochrome P-450 and biomimetic olefin epoxidations is a controversial issue.[2] They are plausible intermediates in reactions between metal alkylidene complexes and carbonyl compounds[3] to yield alkenes, and such reactions have actually been utilized recently for the preparation of 2-metallaoxetanes.[4-6] Various reactions of epoxides with transition metals probably also involve intermediacy of these interesting complexes,[7] although it has recently been shown that epoxide deoxygenations need not involve these intermediates.[6] Oxidative addition of a metal into an epoxide C–O bond to form a metallaoxetane has been proposed in catalytic epoxide rearrangement to ketones,[7b] coupling of epoxides to yield esters,[7c] and metal promoted insertion of CO_2 into epoxides.[7a,m,n] Carbonylation of styrene oxide to a lactone may also involve such an intermediate.[7j] The major transformations involving possible intermediacy of 2-metallaoxetanes are outlined in Scheme I.

Scheme I

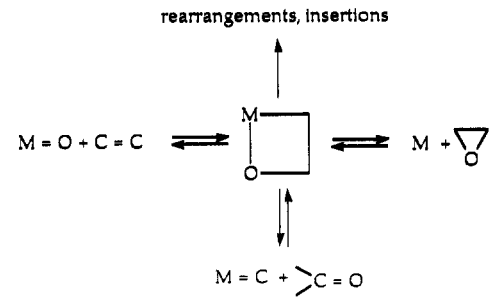

Few metallaoxetanes are known, and of these most have been reported very recently. These interesting molecules were isolated when the ring was stabilized by electron-withdrawing substituents, such as cyano groups in platinum complexes[8] and the pentafluorophenyl group in molybdenum and tungsten compounds.[5] Stabilization is also provided by the presence of an exocyclic double bond, which retards metathetical-type cleavage because of the

† Instituto de Tecnologia Química e Biológica.
‡ Centro de Química Estrutural.
§ Present address: Hacettepe University, Faculty of Engineering, Department of Chemistry, 06532 Beytepe, Ankara, Turkey.

(1) For example: (a) Sharpless, K. B.; Teranishi, A. Y.; Bäckvall, J. E. *J. Am. Chem. Soc.* **1977**, *99*, 3120. (b) Schröder, M.; Constable, E. C. *J. Chem. Soc., Chem. Commun.* **1982**, 734. (c) Rappé, A. K.; Goddard, W. A. *J. Am. Chem. Soc.* **1982**, *104*, 3287. (d) Jørgensen, K. A.; Schiøtt, B. *Chem. Rev.* **1990**, *90*, 1483.

(2) See, for example: (a) Collman, J. P.; Brauman, J. L.; Meunier, B.; Hayashi, T.; Kodadek, T.; Raybuck, S. A. *J. Am. Chem. Soc.* **1985**, *107*, 2000. (b) Collman, J. P.; Kodadek, T.; Raybuck, S. A.; Brauman, J. L.; Papazian, L. M. *Ibid.* **1985**, *107*, 4343. (c) Collman, J. P.; Brauman, J. L.; Meunier, B.; Raybuck, S. A.; Kodadek, T. *Proc. Natl. Acad. Sci. U.S.A.* **1984**, *81*, 3245. (d) Groves, J. T.; Watanabe, Y. *Ibid.* **1986**, *108*, 507. (f) Rappé, A. K.; Goddard, W. A. *Ibid.* **1983**, *204*, 3287.

(3) (a) Tebbe, F. N.; Parshall, G. W.; Reddy, G. S. *J. Am. Chem. Soc.* **1978**, *100*, 3611. (b) Buchwald, S. L.; Grubbs, R. H. *Ibid.* **1983**, *105*, 5490. (c) Pine, S. H.; Zahler, R.; Evans, D. A.; Grubbs, R. H. *Ibid.* **1980**, *102*, 3270. (d) Schrock, R. R. *J. Am. Chem. Soc.* **1976**, *98*, 5399. (e) Aguero, A.; Kress, J.; Osborn, J. A. *J. Chem. Soc., Chem. Commun.* **1986**, 531.

(4) Ho, S. C.; Hentges, S.; Grubbs, R. H. *Organometallics* **1988**, *7*, 780.

(5) Bazan, G. C.; Schrock, R. R.; O'Regan, M. B. *Organometallics* **1991**, *10*, 1062.

(6) Whinnery, L. L., Jr.; Henling, L. M.; Bercaw, J. E. *J. Am. Chem. Soc.* **1991**, *113*, 7575.

(7) (a) De Pasquale, R. J. *J. Chem. Soc., Chem. Commun.* **1973**, 157. (b) Milstein, D.; Buchman, O.; Blum, J. *J. Org. Chem.* **1977**, *42*, 2299. (c) Blum, J.; Zinger, B.; Milstein, D.; Buchman, O. *J. Org. Chem.* **1978**, *43*, 2961. (d) Kamiya, A.; Kawato, K.; Ohta, H. *Chem. Lett.* **1980**, 1549. (e) Schwartz, J.; Hayasi, Y. *Inorg. Chem.* **1981**, *20*, 3473. (f) Suzuki, M.; Watanabe, A.; Noyori, R. *J. Am. Chem. Soc.* **1980**, *102*, 2095. (g) Milstein, D.; Calabrese, J. C. *J. Am. Chem. Soc.* **1982**, *104*, 3733. (h) Osborne, R. B.; Ibers, J. A. *J. Organomet. Chem.* **1982**, *232*, 273. (i) *Ibid.* **1982**, *232*, 371. (j) Alper, H.; Arzoumanian, H.; Petrignani, J.-F.; Saldana-Maldonado, M. *J. Chem. Soc., Chem. Commun.* **1985**, 340. (k) Miyashita, A.; Ishida, J.; Nohira, H. *Tetrahedron Lett.* **1986**, *27*, 2127. (l) Hase, T.; Miyashita, A.; Nohira, H. *Chem. Lett.* **1988**, 219. (m) Aye, K. T.; Ferguson, G.; Lough, A. J.; Puddephatt, R. J. *Angew Chem., Int. Ed. Engl.* **1989**, *28*, 767. (n) Bäckvall, J. E.; Karlsson, O.; Ljunggren, S. O. *Tetrahedron Lett.* **1980**, *21*, 4985.

0276-7333/93/2312-3316$04.00/0

relatively high-energy olefin or ketone that would be produced. Such titanium[4] complexes are known. Simply substituted metallaoxetanes were reported only very recently, including complexes of iridium,[9,10] rhodium[11] (from our laboratories), ruthenium,[12] and tantalum.[6] Crystallographic characterization was also accomplished in a few cases.[5,6,8,11,12b]

In this paper, we describe a straightforward route for the preparation of a rhodaoxetane by oxidative addition of a bromohydrine to a low valent rhodium complex, followed by deprotonation. Both the rhodaoxetane and its precursor were crystallographically characterized, allowing direct evaluation of the structural consequences of ring closure. An account of this work has been communicated.[11] We also show here for the first time that a metallaoxetane can be formed directly by oxidative addition of a simple epoxide to a low valent metal complex. The significance of this result lies in the fact that, by microscopic reversibility, reductive elimination of an epoxide from a metallaoxetane is a feasible process. Such a process has been proposed as a key step in chemical and biomimetic epoxidation of olefins.[1,2] Oxidative addition of Pt(0) to tetracyanoethylene oxide has been described.[11]

Despite the central role that metallaoxetanes play in a variety of processes, not many theoretical studies of such complexes have appeared.[13] Since no other detailed structural characterization of a simple metallaoxetane was available when our studies were carried out, we have theoretically addressed our rhodaoxetane in detail.

Results and Discussion

Our plan for metallaoxetane preparation is shown in eq 1.

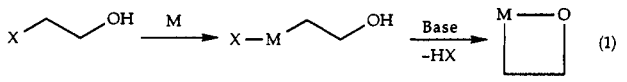

(1)

In order to prevent β-H elimination, we chose to use *gem*-dimethyl substitution, although this was expected to decrease the rate of nucleophilic attack by the metal on C–X. In order to facilitate the oxidative addition reaction, we decided to employ the electron-rich, sterically unhindered $(C_8H_{14})Ir(PMe_3)_3Cl$, **1**. Surprisingly, reaction of **1** with 1-bromo-2-methyl-2-propanol **2** at −30 °C in toluene led to the formation of *mer*-$Ir(PMe_3)_3(H)(Cl)(Br)$, apparently via O–H rather than C–Br activation.[14] By contrast, reaction of **2** with $Rh(PMe_3)_3Cl$ **3** did lead to C–Br oxidative addition. Upon mixing **3** with **2** in toluene at −30 °C, followed by warmup to room temperature, yellow needles were formed, which exhibited an IR absorption at 3361 cm^{-1}, indicating that the O–H group remained intact. ^{13}P NMR revealed a doublet of triplets at 11.7 ppm and a doublet of doublets at −8 ppm, indicating a *mer* configuration. ^1H NMR showed the presence of the hydroxylalkyl moiety, although the CH_2 group could not be observed directly, due to overlap with the PMe_3 protons. This spectral evidence unambiguously shows that C–Br oxidative addition has taken place, although the relative orientation of the halide ligands was not obvious. An X-ray crystallographic study (see below) has confirmed that complex **4** was formed (eq 2). A minor Rh(III) product,

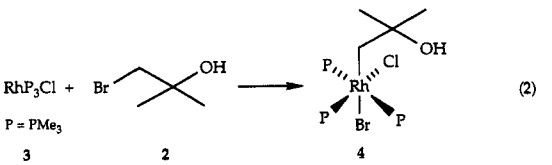

3 2 4 (2)

also containing *mer* arrangement of the phosphine ligands, is also formed. This is likely to be the isomer of **4** in which the halide ligands have exchanged places.

The facility of reaction 2 is surprising in view of the very low reactivity of neopentyl halides in nucleophilic substitution reactions. For example, the average SN^2 rate of ethyl halides is 5 orders of magnitude faster.[15] Indeed, we observed a much slower reaction between **3** and neopentyl bromide, and the facility of reaction 2 may be attributed to assistance by the hydroxy group, perhaps via prior coordination.

Apparently, a very narrow reactivity window exists for reactions of type 2, minor variations in complex and substrate structure having a strong rate effect. Thus, reaction of the bromohydrine **2** with $Rh(PEt_3)_3Cl$ is exceedingly slow, exhibiting 65% unreacted starting material after 3 months at room temperature. This is probably due to a steric effect, which is undoubtedly important in this neopentyl system. Very low reactivity is observed also with $Rh(PMe_3)_4{}^+Cl^-$, probably as a result of lower nucleophilicity of the cationic complex. With the chloro analogue of **2**, 1-chloro-2-methyl-2-propanol, no reactivity is observed with $Rh(PMe_3)_3Cl$ at room temperature. Heating at 65 °C for 5 h resulted in partial decomposition, but the desired oxidative addition product was not formed.

Treatment of the oxidative addition product **4** with the hindered base $(Me_3Si)_2NK$ at −30 °C in the dark led, after filtration, solvent evaporation, and extraction of the residue with benzene, to a meridional complex (by ^{31}P NMR). That deprotonation had occurred was immediately evident from the absence of the hydroxy absorption at 3335 cm^{-1}. After several attempts, it was possible to grow X-ray quality crystals by repeated freeze–thaw concentration of a benzene solution of the product complex. An X-ray crystallographic study (see below) revealed that the rhodaoxetane **5** was formed (eq 3).

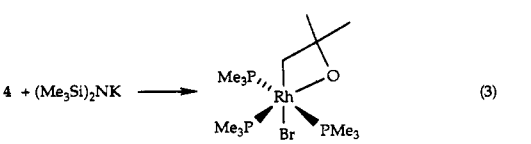

(3)
5

It is interesting that ring closure had resulted in substitution of the chloride rather than the bromide ligand. This may be a result of the strong OH···Cl hydrogen bond

(8) (a) Schlodder, R.; Ibers, J. A.; Lenarda, M.; Graziani, M. *J. Am. Chem. Soc.* **1974**, *96*, 6893. (b) Lenarda, M.; Pahor, N. B.; Calligaris, M.; Graziani, M.; Randaccio, L. *J. Chem. Soc., Dalton Trans.* **1978**, 279. (c) Lenarda, M.; Ros, R.; Traverso, O.; Pitts, W. D.; Baddley, W. H.; Graziani, M. *Inorg. Chem.* **1977**, *16*, 3178.

(9) (a) Klein, D. P.; Hayes, J. C.; Bergman, R. G. *J. Am. Chem. Soc.* **1988**, *110*, 3704. (b) Klein, D. P.; Bergman, R. G. *J. Am. Chem. Soc.* **1989**, *111*, 3079.

(10) Day, V. W.; Klemperer, W. G.; Lockledge, S. P.; Main, D. *J. Am. Chem. Soc.* **1990**, *112*, 2031.

(11) Zlota, A. A.; Frolow, F.; Milstein, D. *J. Am. Chem. Soc.* **1990**, *112*, 6411.

(12) (a) Hartwig, J. F.; Bergman, R. G.; Andersen, R. A. *J. Am. Chem. Soc.* **1990**, *112*, 3234. (b) Idem. *Organometallics* **1991**, *10*, 3344.

(13) (a) Rappé, A. K.; Goddard, W. A. *J. Am. Chem. Soc.* **1980**, *102*, 5114. (b) Bäckvall, J.-E.; Bökman, F.; Blomberg, M. R. A. *J. Am. Chem. Soc.* **1992**, *114*, 534. (c) Cundari, T. R.; Drago, R. S. *Inorg. Chem.* **1990**, *29*, 487.

(14) Zlota, A. A.; Milstein, D. To be published.

(15) March, J. *Advanced Organic Chemistry*, 3rd ed.; Wiley: New York, 1985; pp 88, 298–299.

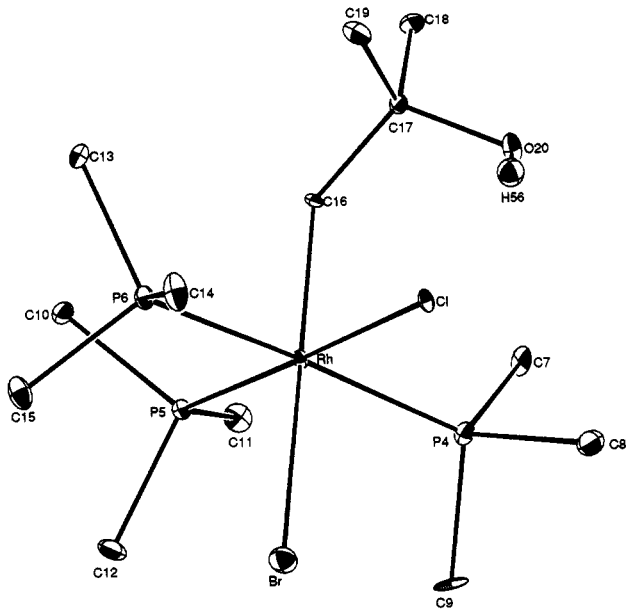

Figure 1. Molecular structure of **4**.

(vide infra). Elimination of HCl is likely to be an SN^i-type reaction, in which formation of Rh–O and rupture of Rh–Cl occur in concert. Attack at the metal followed by chloride expulsion is unlikely at this saturated metal center.

We reported that complexes **1** and **3** react with epoxides to yield β-oxoalkyl complexes **6**, presumably via oxidative addition of the epoxide C–O bond, followed by β-H elimination[7g,16] (eq 4).

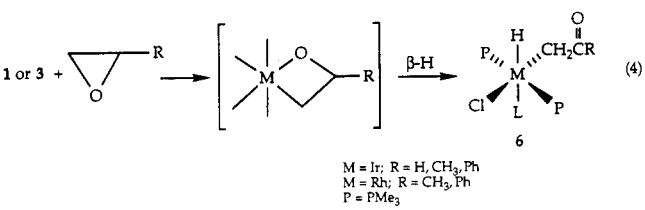

(4)

Complexes **6** (M = Rh), which undergo C–H reductive elimination of the corresponding ketones, are intermediates in the catalytic isomerization of epoxides.[16] Attempting to isolate the postulated metallaoxetane intermediate, we utilized β,β-disubstituted epoxides in order to prevent β-H elimination. However, mixtures resulted. Upon reexamination of these reactions, we have now discovered that reaction of $Rh(PMe_3)_3Br$ with isobutylene oxide results in the formation of the rhodaoxetane **5** in ca. 30% yield (eq 5).

(5)

This result is of considerable significance since it indicates, for the first time, that (a) oxidative addition of simple epoxides to yield metallaoxetanes is indeed a viable step in metal promoted reactions of epoxides and (b) by microscopic reversibility the reductive elimination of an epoxide from a metal complex is a feasible process. This controversial step has been proposed in transition metal catalyzed epoxidations of olefins, including cytochrome P-450 and biomimetic catalysis.[2]

Structures. The structures of complexes **4** and **5** were solved by automated Patterson analysis and the Fourier method. Drawings of the molecular structures appear in

(16) Milstein, D. *J. Am. Chem. Soc.* **1982**, *104*, 5227.

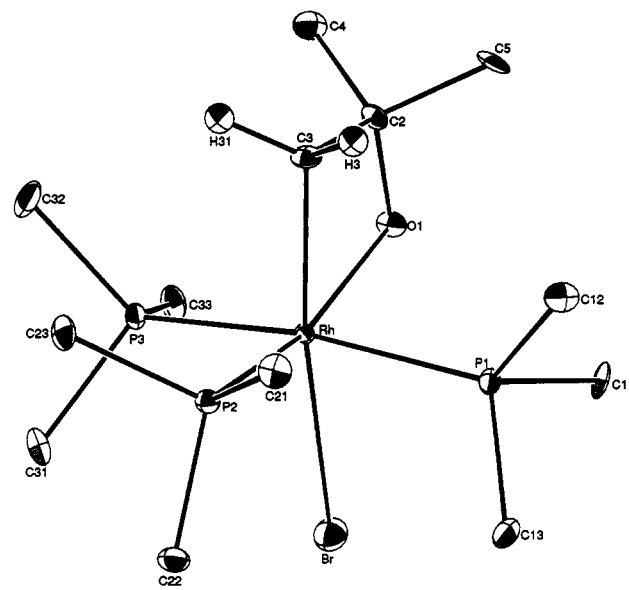

Figure 2. Molecular structure of **5**.

Table I. Experimental Crystallographic Data for 4 and 5

	complex **4**	complex **5**
mol wt	519.61	483.15
space group	$P2_1/c$ (monoclinic)	$P2_12_12_1$ (orthorhombic)
temp, °C	−183	−183
cell constants		
a, Å	16.418(9)	15.069(2)
b, Å	8.972(9)	15.525(2)
c, Å	14.375(9)	8.662(4)
cell vol, Å^3	2117(2)	2026(1)
formula	$C_{13}H_{36}OP_3ClBrRh$	$C_{13}H_{35}OP_3BrRh$
formula units/unit cell	4	4
D(calcd), g cm^{-3}	1.63	1.58
μ(calcd), cm^{-1}	30.11	30.10
diffractometer/scan	Rigaku AFC5/ω–2θ	Rigaku AFC5/ω
source rotating anode	Rigaku RU300	Rigaku RU300
speed of measmt, deg min^{-1}	32	4
radiation, graphite monochr	Mo Kα	Mo Kα
max cryst dimens, mm	0.10 × 0.10 × 0.10	0.30 × 0.30 × 0.10
no. of reflections		
measd	4648	6384
duplicates	429	3194
with $F_o > 3\sigma(F_o)$	3156	2613
θ_{max}, deg	27	27.5
final R, R_w	0.044, 0.046	0.042, 0.044

Figures 1 and 2, experimental crystallographic data appear in Table I, and intramolecular bond distances and angles appear in Tables II and III. It can be clearly seen that complex **4** is the trans-oxidative addition product of the bromohydrine **2** to complex **3**. Coordination around the rhodium is octahedral with very little distortion. Rh–P(5) is 0.1 Å shorter than Rh–P(4) or Rh–P(5), a manifestation of the weak chloride trans influence. The OH···Cl distance of 2.462(0.078) Å indicates a strong intramolecular hydrogen bond, as reported also for other metal-bound halide ligands.[17] The O–H–Cl angle is 152.47-(8.44)°. Formation of this hydrogen bond has an undoubtedly important role in the determination of the stereochemistry of the thermodynamic product complex, as has been observed in other cases involving iridium amine complexes.[17]

Crystallographic characterization of the rhodaoxetane **5** and structural comparison with its precursor **4** allows direct evaluation of the structural consequence of ring closure. Coordination around the rhodium atom remains

(17) For other recently reported intramolecular hydrogen bonds involving a halogen ligand, see: Fryzuk, M. D.; MacNeil, P. A.; Rettig, S. J. *J. Am. Chem. Soc.* **1987**, *109*, 2303.

Table II. Bond Distances (Å) and Angles (deg) for 4

Bond Distances

Rh(1)–Br(2)	2.661(4)	Rh(1)–Cl(3)	2.485(4)
Rh(1)–P(4)	2.367(4)	Rh(1)–P(5)	2.271(4)
Rh(1)–P(6)	2.367(4)	Rh(1)–C(16)	2.131(8)
P(4)–C(7)	1.832(9)	P(4)–C(8)	1.823(10)
P(4)–C(9)	1.823(10)	P(5)–C(10)	1.820(9)
P(5)–C(11)	1.824(9)	P(5)–C(12)	1.819(9)
P(6)–C(13)	1.829(9)	P(6)–C(14)	1.803(10)
P(6)–C(15)	1.829(9)	C(16)–C(17)	1.542(11)
C(17)–C(18)	1.519(11)	C(17)–C(19)	1.529(12)
C(17)–O(20)	1.452(9)		

Bond Angles

Br(2)–Rh(1)–Cl(3)	85.3(1)	Br(2)–Rh(1)–P(4)	88.1(1)
Cl(3)–Rh(1)–P(4)	88.4(2)	Br(2)–Rh(1)–P(5)	95.1(1)
Cl(3)–Rh(1)–P(5)	178.6(1)	P(4)–Rh(1)–P(5)	93.0(2)
Br(2)–Rh(1)–P(6)	86.1(1)	Cl(3)–Rh(1)–P(6)	87.0(2)
P(4)–Rh(1)–P(6)	172.9(1)	P(5)–Rh(1)–P(6)	91.7(2)
Br(2)–Rh(1)–C(16)	178.5(2)	Cl(3)–Rh(1)–C(16)	96.0(3)
P(4)–Rh(1)–C(16)	91.2(3)	P(5)–Rh(1)–C(16)	83.6(3)
P(6)–Rh(1)–C(16)	94.7(3)	Rh(1)–P(4)–C(7)	120.4(3)
Rh(1)–P(4)–C(8)	114.7(4)	C(7)–P(4)–C(8)	100.8(5)
Rh(1)–P(4)–C(9)	114.4(4)	C(7)–P(4)–C(9)	103.5(5)
C(8)–P(4)–C(9)	100.4(5)	Rh(1)–P(5)–C(10)	117.1(3)
Rh(1)–P(5)–C(11)	119.5(3)	C(10)–P(5)–C(11)	97.1(4)
Rh(1)–P(5)–C(12)	116.2(4)	C(10)–P(5)–C(12)	102.8(4)
C(11)–P(5)–C(12)	100.8(4)	Rh(1)–P(6)–C(13)	120.2(3)
Rh(1)–P(6)–C(14)	114.0(3)	C(13)–P(6)–C(14)	102.1(4)
Rh(1)–P(6)–C(15)	116.4(3)	C(13)–P(6)–C(15)	102.1(4)
C(14)–P(4)–C(15)	99.0(4)	Rh(1)–C(16)–P(17)	123.2(5)
C(16)–C(17)–C(18)	108.6(6)	C(16)–C(17)–C(19)	112.3(6)
C(18)–C(17)–C(19)	108.2(7)	C(16)–C(17)–O(20)	112.1(6)
C(18)–C(17)–O(20)	108.2(7)	C(19)–C(17)–O(20)	109.8(6)

Table III. Bond Distances (Å) and Angles (deg) for 5

Bond Distances

Rh(1)–Br(2)	2.613(4)	Rh(1)–P(1)	2.352(4)
Rh(1)–P(2)	2.255(4)	Rh(1)–P(3)	2.331(4)
Rh(1)–O(1)	2.099(8)	Rh(1)–C(3)	2.069(10)
P(1)–C(11)	1.837(11)	P(1)–C(12)	1.822(11)
P(1)–C(13)	1.830(11)	P(2)–C(21)	1.808(11)
P(2)–C(22)	1.816(11)	P(2)–C(23)	1.844(12)
P(3)–C(31)	1.833(11)	P(3)–C(32)	1.815(11)
P(3)–C(33)	1.808(11)	O(1)–C(2)	1.416(12)
C(2)–C(3)	1.537(14)	C(2)–C(4)	1.516(15)
C(2)–C(5)	1.539(14)		

Bond Angles

P(1)–Rh(1)–Br(2)	83.5(2)	Br(2)–Rh(1)–P(2)	99.1(2)
P(1)–Rh(1)–P(2)	93.3(2)	Br(2)–Rh(1)–P(3)	83.7(2)
P(1)–Rh(1)–P(3)	166.1(1)	P(2)–Rh(1)–P(3)	94.0(2)
O(1)–Rh(1)–Br(2)	97.3(3)	O(1)–Rh(1)–P(1)	87.9(3)
O(1)–Rh(1)–P(2)	163.6(2)	O(1)–Rh(1)–P(3)	88.4(3)
Br(2)–Rh(1)–C(3)	165.0(2)	P(1)–Rh(1)–C(3)	96.1(3)
P(2)–Rh(1)–C(3)	96.0(3)	P(3)–Rh(1)–C(3)	94.8(3)
O(1)–Rh(1)–C(3)	67.6(4)	Rh(1)–P(1)–C(11)	109.9(4)
Rh(1)–P(1)–C(12)	123.9(4)	C(11)–P(1)–C(12)	102.6(5)
Rh(1)–P(1)–C(13)	116.1(4)	C(11)–P(1)–C(13)	101.0(5)
C(12)–P(1)–C(13)	100.2(5)	Rh(1)–P(2)–C(21)	116.0(4)
Rh(1)–P(2)–C(23)	116.1(4)	C(21)–P(2)–C(22)	103.4(5)
C(22)–P(2)–C(23)	102.3(5)	C(21)–P(2)–C(23)	97.9(5)
Rh(1)–P(3)–C(32)	123.5(5)	Rh(1)–P(3)–C(31)	116.3(4)
Rh(1)–P(3)–C(33)	110.4(4)	C(31)–P(3)–C(32)	100.2(6)
C(32)–P(3)–C(33)	102.8(6)	C(31)–P(3)–C(33)	100.5(5)
O(1)–C(2)–C(3)	103.5(7)	Rh(1)–O(1)–C(2)	95.7(5)
C(3)–C(2)–C(4)	113.6(8)	O(1)–C(2)–C(4)	111.5(8)
C(3)–C(2)–C(5)	111.9(8)	O(1)–C(2)–C(5)	109.8(8)
Rh(1)–C(3)–C(2)	93.2(6)	C(4)–C(2)–C(5)	106.6(8)
Rh(1)–C(3)–H(31)	113.3(8)	Rh(1)–C(3)–H(31)	113.5(8)

octahedral, with Rh–P(2) being shorter than Rh–P(1) or Rh–P(3), reflecting the small trans influence of the alkoxy ligand relative to that of PMe_3. As a matter of fact, comparison of **4** with **5** reveals that the trans effect of the (cyclo)alkoxy ligand is even smaller than that of the chloride ligand.

Significantly, the structure clearly shows the presence of an essentially planar rhodaoxetane ring, deviation of the atoms from the Rh–O–C(3)–C(2) plane being effectively 0. The dihedral angle between, e.g., the C(2)–C(3)–O and O–Rh–C(3) planes is 0.3°, less than the standard deviation (1.5°). An essentially flat ruthenaoxetane ring (containing an exocyclic double bond) with a dihedral angle of 1.9° was also reported very recently.[12] Although less relevant, 3-oxaplatinacyclobutanes also exhibit a planar ring.[18]

On the basis of solution NMR studies, it was concluded that a 3-methylenetitanaoxetane is considerably puckered in order to obtain optimal orbital overlap involving donation of the oxygen lone pair to an empty a_1 orbital.[4] Puckering of a molybdaoxetane ring (21.3°) has been attributed to a characteristic distortion of square pyramidal group 6 metallacyclobutanes.[5] Crystallographic characterization of $Cp_2^*(CH_3)Ta(OCH_2CHPh)$[6] shows a puckered ring (25.2°), attributed to unfavorable steric interaction involving the phenyl substituent and the Cp* ligand. Cyano-substituted platinaoxetanes exhibit a considerably puckered ring, the dihedral angle being as large as 30°.[8b] This could be due to an unfavorable staggered conformation of the cyano groups in a planar ring, or perhaps to interaction of a cyano group with the metal. A puckering angle of 15.8° was also found in a rhenium derivative.[19]

In conclusion, the structure data suggest that in the absence of steric interactions, when a saturated metal center which cannot interact with the oxygen lone pair or a substituent on the ring is involved, a planar ring is expected.

Comparison of the structures **4** and **5** shows that both Rh—C and C—O bonds are significantly shorter in the rhodaoxetane. As a matter of fact, the C—O bond of **5** is even shorter than that of oxetane itself, reported to be 1.444(2) Å.[20] This is contrary to the expectation of increased bond length upon strain relief.[8a,21] These features indicate some contribution of structure **7**, in which

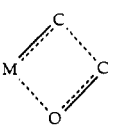

7

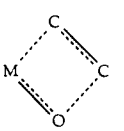

8

partial "metathesis" to a metal carbene and a ketone has taken place. Indeed, complex **5** has the shortest M—C bond (2.069 Å) of the reported metallaoxetanes. Structure **7** may be characteristic of late transition metallaoxetanes, whereas, for the oxophilic early metals, structure **8** may be more important. In accordance with this, the Rh complex **5** and the structurally characterized ruthenaoxetane[12] have C—O and longer C—C bonds somewhat shorter than those reported for the Mo[5] and Ta[6] complexes. Manifestation of this in reactivity is exemplified in the photoextrusion of a ketone from an iridaoxetane[9b] and decomposition of the Ta[6] and Mo[5] oxetanes to yield M=O and the corresponding olefins.

(18) (a) Hoover, J. F.; Stryker, J. M. *J. Am. Chem. Soc.* **1989**, *111*, 6466. (b) Idem. *Organometallics* **1989**, *8*, 2973.

(19) Herrmann, W. A.; Kusthardt, U.; Schafer, A.; Herdtweck, E. *Angew. Chem., Int. Ed. Engl.* **1986**, *25*, 817.

(20) Chan, S. I.; Zinn, J.; Gwinn, W. D. *J. Chem. Phys.* **1961**, *34*, 1319.

(21) For example, the C–O bond length of oxirane is slightly shorter than that of oxetane; see ref 19 and: Cunningham, G. L.; Boyd, A. W.; Myers, R. J.; Gwinn, W. D.; LeVan, W. J. *J. Chem. Phys.* **1951**, *19*, 676.

Molecular Orbital Calculations. The structural features of the rhodaoxetane complex raised a number of interesting questions, namely the origin of the planarity of the metallaoxetane ring and the existence of relatively short Rh–C and C–O bonds. Extended Hückel[22] molecular orbital calculations were used to study the bonding in the complex and to try to understand qualitatively its reactivity. The model compound is a distorted octahedral *mer*-$(PH_3)_3BrRh(OCH_2CH_2)$ (further details are in the Experimental Section), taken from the X-ray structure of **5**.

Rhodaoxetane. The interaction between a Rh(III) d^6 ML_4 fragment and the OCH_2CH_2 ligand is shown schematically below for two limiting situations. In the first one, **9**, the Rh–O–C–C ring is planar, while in **10** it is puckered (the puckering angle, α, is the angle between the C–Rh–O and C–C–O planes).

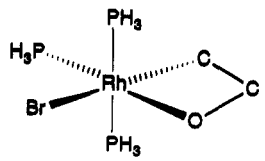

9

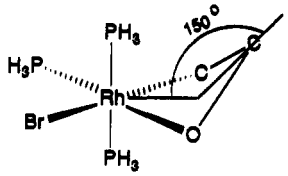

10

The change in total energy accompanying the bending of the metallacycle across the central C–O bond is shown in Figure 3. Although the potential energy surface is relatively flat for small bending angles, the planar ring is preferred.

To understand why this happens, an analysis of the bonding in the complex is helpful. The frontier orbitals of an ideal C_{2v} ML_4 d^6 fragment[23] are shown in **11** in relation to those of the parent octahedron.

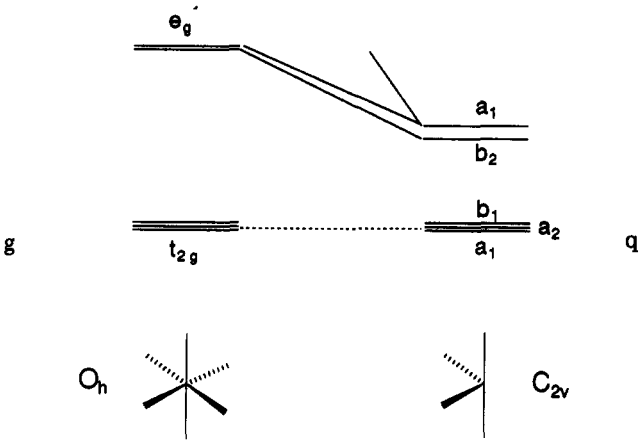

11

The loss of two equatorial ligands is more acutely felt in the strongly antibonding e_g^* orbitals, which become more stable. Mixing of empty high energy levels, made possible by the lower symmetry, enhances this effect, giving rise especially to the sp hybrid $2a_1$. These frontier orbitals are present almost essentially unaltered, in spite of the even lower symmetry of $RhBr(PH_3)_4^{2+}$, in the center of the molecular orbital diagram of Figure 4. On the left and right sides are shown the orbitals of the open fragment

(22) (a) Hoffmann, R. *J. Chem. Phys.* **1963**, *39*, 1397. (b) Hoffmann, R.; Lipscomb, W. N. *J. Chem. Phys.* **1962**, *37*, 2179.
(23) Albright, T. A.; Burdett, J. K.; Whangbo, M.-H. *Orbital Interactions in Chemistry*; Wiley-Interscience: New York, 1985.

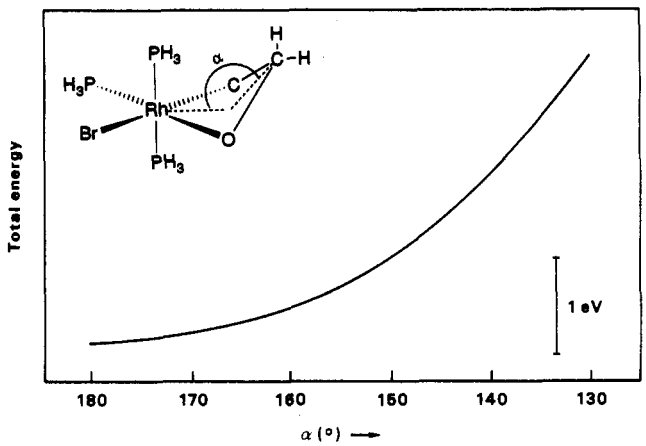

Figure 3. Change in total energy of complex $(PH_3)_3BrRh(OCH_2CH_2)$ while bending the ring.

$CH_2CH_2O^{2-}$, with the oxygen atom lying on the *y* axis, which interact with those of the metallic fragment, to give both the planar ring rhodaoxetane **9** (right side) and the bent one, **10** (left side).

Most of the energy levels do not change significantly from right to left in the diagram. Notice that bending the Rh–O–C–C cycle removes the only symmetry element present in planar metallacycle **9**. The HOMO and the second HOMO (initially *xy* and *yz*, respectively) are both destabilized. They mix and their character is almost reversed. As a matter of fact, the HOMO of **10**, the puckered metallacycle, is essentially *yz*, while *xy* contributes most to the second HOMO. In a simplified way, the essential features of the Walsh diagram are as shown in **12**. The destabilization of *yz* which acquires a strong π antibonding character is mostly responsible for the higher energy of the puckered geometry.

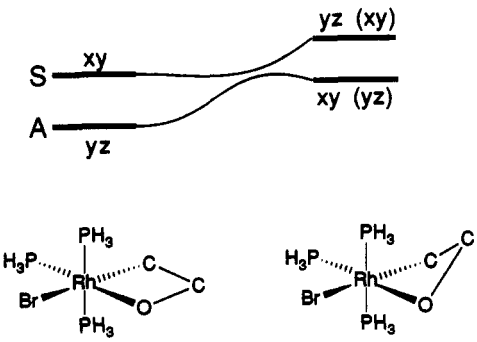

12

The bonding in **9** (right side of Figure 4) has three main components: donation of electrons from carbon and from oxygen to the two empty orbitals of Rh, forming the two σ bonds, and a weak π type four-electron destabilizing interaction between *xy* and the other oxygen lone pair in the *xy* plane. When the ring bends, the total overlap population between the two fragments $(RhBr(PH_3)_3^{2+}$ and $CH_2CH_2O^{2-})$ drops from 0.34 to 0.21, indicating that weaker bonds are formed. This can be accounted for by two separate effects: first, there is a decreased overlap between the carbon and oxygen orbitals, which are now differently oriented, and the empty orbitals of the metallic fragment lying in the *xy* plane; second, the overlap between the oxygen orbitals and filled orbitals of Rh (*xy* and *yz*) increases, leading to a more repulsive interaction. Owing to the very low symmetry of the puckered rhodaoxetane,

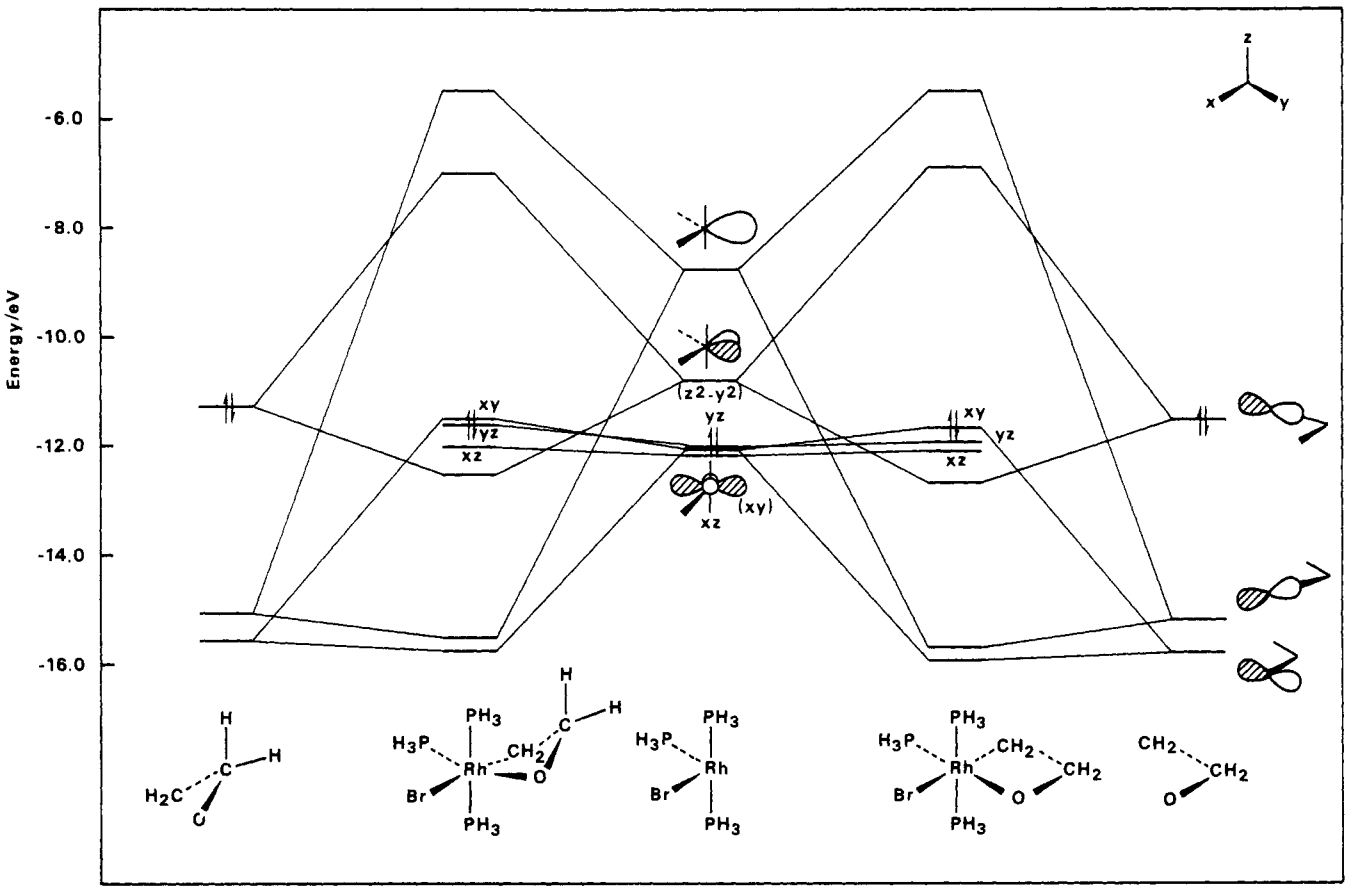

Figure 4. Interaction diagram between the d^6 $(PH_3)_3BrRh$ fragment and $OCH_2CH_2^{2-}$ to form a planar (right side) or a bent (left side) metallacycle ring.

all levels are mixed and it is difficult to see these effects clearly separated in the molecular orbital diagram.

There has been some discussion concerning the planarity of four-membered metallaoxetane rings,[24] but not many structures were found.[25] With the exception of the rhodaoxetane and a ruthenium derivative containing an sp^2 carbon,[12] the rings were found to be puckered in the solid, as described in more detail earlier. Interestingly, ab initio results indicate that the titanaoxetane isolated by Grubbs and co-workers and thought to be puckered,[4] might be planar.[26] We suggest, therefore, that planarity is electronically preferred but quite often has to be avoided for steric reasons.

An analysis of the overlap populations inside the Rh–O–C–C ring was done. Results are schematically shown in **13** for both geometries of the rhodaoxetane.

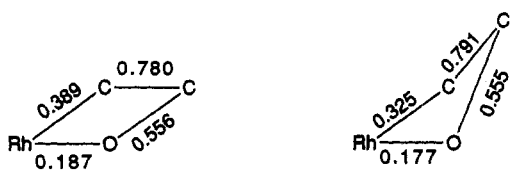

13

They indicate that the planar geometry is more stable because stronger metal–ligand bonds can be formed. Overlap populations are a useful measure of bond strength but they should be used with caution and only in terms of relative values. How does the C–C bond in the cycle compare for instance, with another C–C bond? The C–C overlap population in ethylene oxide is only 0.66, and others are given in **14** (all calculations were done with C–C 1.54

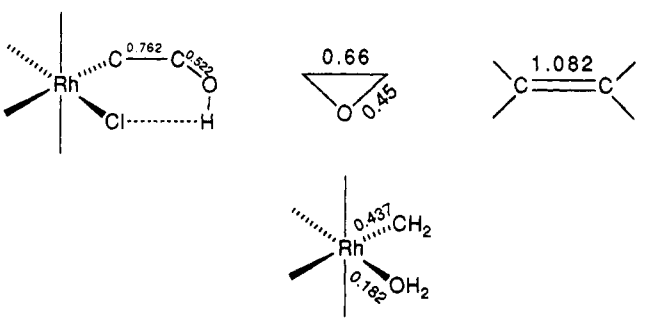

14

Å, except ethylene oxide with 1.47 Å). The C–C bond in the metallacycle is then slightly stronger than a single bond and much stronger than that in the strained ethylene oxide. It is more difficult to compare Rh–C and Rh–O bonds with others. For instance, in the carbene model $Rh(PH_3)_3Br(CH_2)(OCH_2)$, Rh–C and Rh–O overlap populations are respectively 0.635 and 0.281.

These numbers indicate a relatively weak Rh–O bond in the metallacycle. In the related model compounds $Rh(PH_3)_3Br(CH_2)(OH_2)$ and $Rh(PH_3)_3Br(CH_3)(OH)$, Rh–C and Rh–O overlap populations are respectively 0.437, 0.182 and 0.424, 0.216. The formulation **7** above is thus consistent with this proposed bonding model.

Metathesis: Formation of a Ketone or an Alkene? The previous bonding model suggests that the metallacycle

(24) Schiøtt, B.; Jørgensen, K. A.; Calhorda, M. J.; Galvão, A. M. *Organometallics* **1992**, *11*, 4213.
(25) Allen, F. H.; Kennard, O.; Taylor, R. *Acc. Chem. Res.* **1983**, *16*, 146.
(26) Schiøtt, B.; Jørgensen, K. A. Unpublished results (from ref 24).

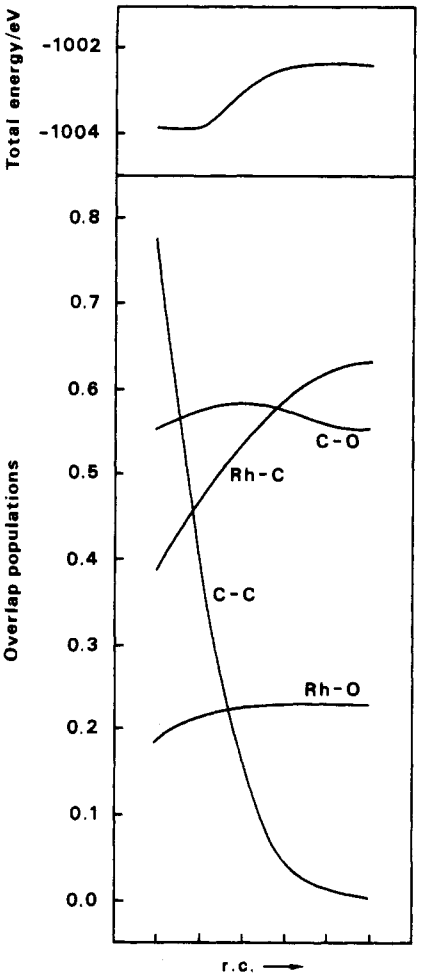

Figure 5. Change in total energy and overlap populations along the reaction path described in **15**.

with a stronger M–C bond and a relatively weak M–O bond might be considered as initiating a methathesis reaction, to form a ketone, leaving behind a metal–carbene fragment, as sketched in **15**.

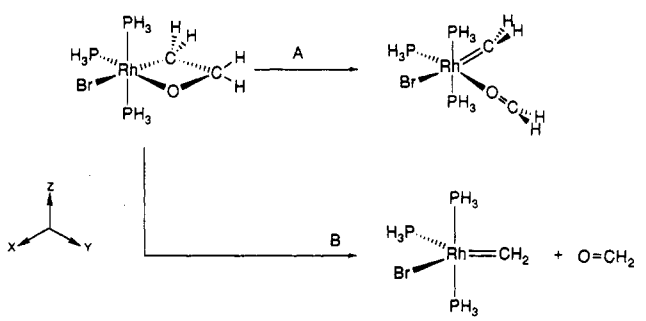

15

Such reactions are rare, the only known example being the photoextrusion of a ketone from an iridium complex with isolation of the resulting carbene complex $IrCp^*PMe_3(CH_2)$,[9b] and the likelihood of its occurrence in competition with the better known methathesis to give alkenes,[6] as shown in **16**, was thus investigated. The thermodynamics of these reactions was theoretically studied for Cr and Mo complexes in high formal oxidation states,[13a] the results being different for each metal. While for Mo the metallacycle was the most stable form, Cr preferred to decompose to give $CrCl_2O_2$ and ethylene. Decomposition products $MCl_2O(CH_2)$ and $O(CH_2)$ had very high energies for Mo and Cr. A second study[13b] dealt with reactions of the naked metals. Decomposition of the metallacycle into

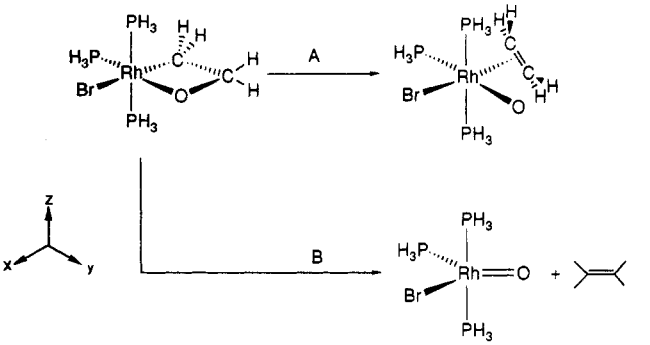

16

$O(CH_2)$ and $M{=}CH_2$ is not addressed, but on the other hand, for both Mo and Cr, that structure is thermodynamically stable relative to M=O and ethylene. The difficulty of extracting from these studies information which might be relevant to our system (intermediate formal oxidation state, other ligands) led us to analyze the reactions under the same conditions, despite the limitations of extended Hückel calculations.

In reaction path A the symmetry plane (containing Br, P, Rh, O, C) is kept during reaction. Among four limiting conformations possible for the final product, which differ by the relative positions of the methylene protons, the one shown in **15** is the most stable, as it minimizes interligand repulsions. It is also compatible with C_s symmetry.

The activation energy for this reaction is 1.5 eV (~35 kcal mol^{-1}), but the final product is not particularly stable. On the other hand, while the Rh–C bond becomes stronger, consistent with formation of a metal–carbene bond, the same does not happen with the C–O bond, which remains weak. The Rh–O bond, which had been found to be very weak both in the calculations and from the structural evidence, becomes slightly stronger, and as expected, the C–C overlap population drops to zero as this bond breaks. These results derive from the presence of two electrons in two antibonding levels which are very close in energy (C–O π^* and Rh–C π^*). The complex should be more stable for a system containing two less electrons with these two levels empty. In conclusion, the activation energy for this process is relatively low, but the final product is unstable. This agrees with the results of the earlier theoretical studies, for both Cr and Mo.[13a] Releasing the ketone, as in pathway B (**15**), leads to no major change.

Metathesis reactions of the type shown in **16** are known[6] and its inverse has been studied in several contexts.[27] The metallacycle can open by breaking a C–O bond, so that an olefin and Rh–O are formed, and may end with the olefin coordinated to rhodium (A), or with the olefin leaving the metal (B), **16**. To study reaction A, the C–O bond was allowed to break (increasing d1), while the C–C group rearranged itself (midpoint of the C–C bond, D, moving closer to Rh, d2), in such a way that the symmetry plane was kept, **17** (the methylene hydrogens are omitted). The D–Rh–O angle was optimized.

The reaction is very favorable from the point of view of energy. While the Rh–oxygen overlap population increases slightly, the product has two strong Rh–C bonds (instead

(27) (a) Friend, C. M.; Roberts, J. T. *Acc. Chem. Res.* **1988**, *21*, 394. (b) Friend, C. M.; Roberts, J. T. *J. Am. Chem. Soc.* **1987**, *109*, 7899. (c) Friend, C. M.; Roberts, J. T. *J. Am. Chem. Soc.* **1987**, *109*, 3872. (d) Friend, C. M.; Roberts, J. T. *J. Am. Chem. Soc.* **1986**, *108*, 7204. (e) Calhorda, M. J.; Hoffmann, R.; Friend, C. M. *J. Am. Chem. Soc.* **1990**, *112*, 50.

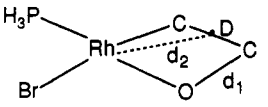

17

of only one, although stronger) and the internal C–C bond also becomes stronger, taking on some double bond character, as expected from a coordinated olefin. Notice, however, that the C–C overlap population is ca. 0.9, while for free ethylene with the same geometry, it should be closer to 1.1. This reflects the bonding mode of an ethylene molecule to a transition metal. Both donation from π to the LUMO of $RhBr(PH_3)_3^{2+}$ and back-donation from xy to π^* contribute to weaken the C–C bond, in the classical model of Chatt–Dewar–Duncanson.[28]

From an electronic point of view, this complex looks much more likely to be stable than the carbene derivative discussed in the previous section. There is a convenient HOMO–LUMO gap and no strong four electron destabilizing interactions. Comparing the final product to the parent rhodaoxetane, we can assign its lower energy (ca. 1 eV) to the stabilization of the "t_{2g}" orbitals. While xy and yz were slightly π antibonding, xy becomes now bonding through back-donation to π^*, and yz stays mainly nonbonding. The stabilization of xy along the reaction coordinate is partly responsible for the shape of the total energy curve and obscures any activation barrier which certainly exists. This will come from breaking the C–O bond: bonding levels lose their bonding character, becoming higher in energy. This previous reaction ends with a distorted octahedral Rh(III) complex: in the alternative path B, the olefin becomes free during the reaction and the final complex has coordination number 5, for which a trigonal bipyramidal geometry was considered. The final products have lower energy (0.1 eV) than those in path A. Although the Rh bond to C=C is lost, stronger bonds between the metal and the five ligands (specially the oxo ligand) can now be formed. The C—C bond in the olefin acquires its double bond character, as reflected in an increased overlap population. In this case, it is the formation of the C=C bond which is the driving force for the reaction, while a barrier should be provided by breaking the C—O bond.

These results are probably biased by using the extended Hückel approach, but as pointed out above, more sophisticated types of calculation led to inconclusive results; namely, they do not always predict the metallacycle to be more stable than ethylene plus some metal oxide.[13] Recall, however, that these last products were, in all cases, more stable than metal carbene plus formaldehyde and this is also found in our results. In spite of the relative strength of internal bonds in the metallacycle, **7**, an alkene will more likely be formed than OCH_2 from the competing reaction.

Reductive Elimination of Epoxide. This possibility is interesting to address, since the reverse reaction was experimentally found to take place (see eq 5, above). The simplest way of forming the epoxide is shown in 18, without

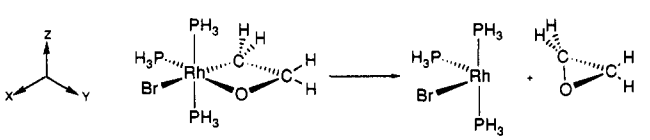

18

relaxation of the organometallic fragment left behind after loss of the epoxide and keeping the symmetry plane. The C–O bond starts to form at the same time that the carbon atom opposite Rh is allowed to move away from the metal, until it is 2 Å away, a distance for which no interaction is found between ethylene oxide and the $RhBr(PH_3)_3^{2+}$ fragment. While the hydrogen atoms have to reorient, no further bond lengths are changed.

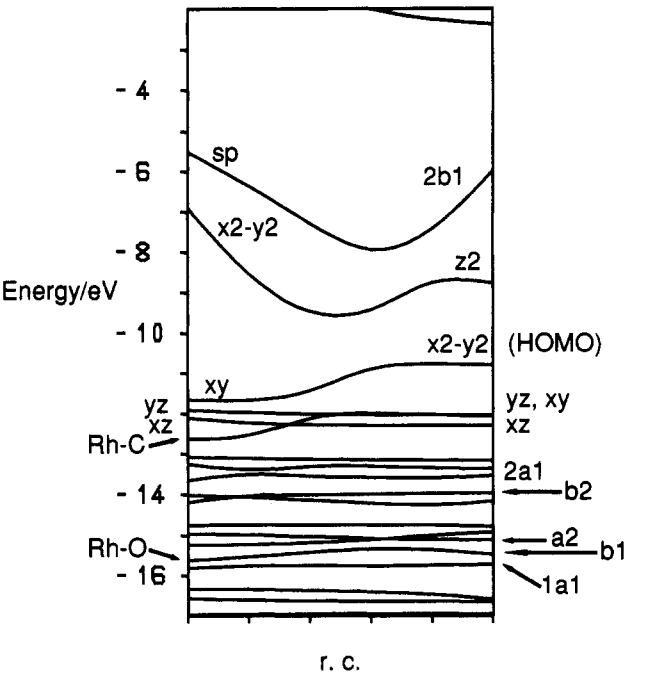

Figure 6. Walsh diagram for the reaction shown in 18.

The activation energy for this reaction is relatively high (ca. 3.6 eV), and the overlap populations change as expected: the C–O overlap population increases, while both Rh–C and Rh–O drop to zero. The high barrier is caused by the high energy of the sawhorse geometry of the final Rh complex and also by the fact that the reaction is formally a forbidden one. The Walsh diagram in Figure 6 shows clearly an avoided crossing: the LUMO, $x^2 - y^2$, becomes the HOMO in the final species. Also represented at the final step of this Walsh diagram are the levels of ethylene oxide, schematized in 19.

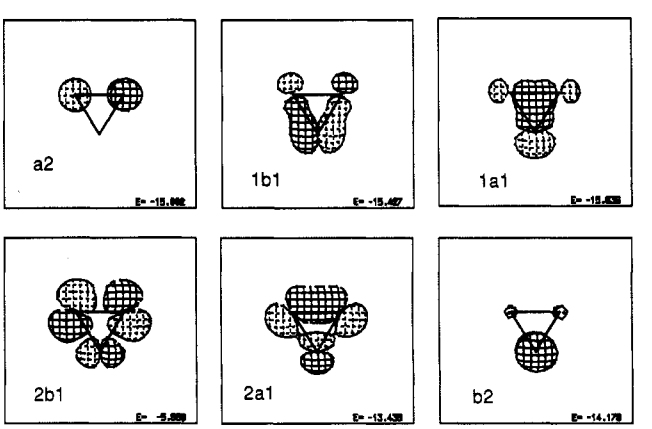

19

A major contribution to the activation barrier arises from breaking the two bonds, Rh–C and Rh–O. The two bonding molecular orbitals (Rh–C, Rh–O in Figure 6) which can be assigned to these bonds are destabilized as their

bonding character is lost, and they end up at relatively high energies.

If the four coordinate Rh(I) d^8 complex is allowed to become square planar, the energy of the final state drops by almost 1 eV and a smaller barrier may be expected accordingly. A slightly different pathway was also tried, in which ethylene oxide formed but stayed coordinated to the metal, but without major differences.

The Walsh diagram in Figure 6 shows the HOMO to be greatly destabilized during the reductive elimination reaction. One might expect, therefore, that photochemical activation, promoting one electron from the HOMO to the LUMO, which goes down in energy, would enhance the reaction. This would be, in a way, a form of acting on the reactant. Others can be envisaged, such as removing one of the ligands, Br or phosphine, in the initial complex. Two sets of calculations were thus performed starting from the pentacoordinated intermediates $RhX(PH_3)_2(OC_2H_4)$ with X = Br or PH_3. Assuming that the reaction takes place in one step (A), with ethylene oxide forming and moving away from the metal at the same time, the barrier drops to 2.7 eV (X = Br) or 2.5 eV (X = PH_3). For path B, they drop even further (to 1.8 and 1.7 eV, respectively).

These results are in accordance with a main idea obtained from other theoretical studies,[13] which is that the metallacycle geometry is normally much more stable than epoxide plus metal fragment, and also with the availability of the pathway for the reverse reaction.

Conclusions

The rhodaoxetane complex **5** described in this work shows a planar Rh–O–C–C ring. This geometry is favored from an electronic point of view, as the four electron π repulsive interactions between filled orbitals of rhodium and oxygen are avoided and there are no steric constraints to force the ring away from planarity. The role of this complex as an intermediate in several reactions (Scheme I) was investigated in view of the current interest in metallacycles as suitable intermediates. The results are in relatively good agreement with those from better quality calculations, as far as they can be compared, considering the different types of chemical systems handled. Decomposition to alkenes appears as the preferred decomposition pathway, while the study of the reductive elimination reaction helped to understand the formation of the metallacycle from the epoxide.

Experimental Section

Molecular Orbital Calculations. All calculations were of the extended Hückel type[22] with modified H_{ij}'s.[29] The basis set for the metal consisted of ns, np, and (n – 1)d orbitals. The s and p orbitals were described by single Slater-type wave functions, and the d orbitals were taken as contracted linear combinations of two Slater-type wave functions.

The geometry of the model Rh complex was taken from the structure of complex **5**. The environment around the metal was a distorted octahedron, with two axial PH_3 groups and the Br *cis* relative to the O of the ring. The oxygen atom was lying on the *y* axis, and the experimental value of the O–Rh–C angle was taken (67.6°). The distances were not changed except when mentioned in the text.

Standard parameters were used for C, H, O, P, and Br, while those for rhodium are the following (orbital, H_{ii}/eV, ζ): 5s –8.09, 2.135; 5p –4.57, 2.100; 4d –12.50, 4.29, 1.97 (ζ2), 0.5807 (C_1), 0.5685 (C_2). The three dimensional representation of the molecular orbitals of ethylene oxide (**19**) was made using the program CACAO.[30]

General Procedures. All reactions were carried out under nitrogen in a Vacuum Atmospheres glovebox equipped with a recirculation "Dri Train" or using Schlenk techniques. Solvents were dried, distilled, and degassed before introduction into the glovebox, where they were stored over activated 4-Å molecular sieves. Reaction flasks were washed with water and acetone and oven dried before introducing them into the glovebox.

Spectroscopic Analysis. NMR spectra were recorded on Bruker WH-270 or AM-500 instruments. ^1H nuclei were observed at 270 or 500 MHz; ^{31}P nuclei were observed at 109.294 MHz (with ^1H decoupling). IR spectra were recorded in Nujol mulls on KBr plates on a Matteson Cygnus-25 or on a Nicolet MX-1 spectrometer. ^1H NMR chemical shifts are relative to tetramethylsilane; the residual solvent peak was used as an internal reference. ^{31}P NMR chemical shifts are relative to 85% H_3PO_4 at δ 0.0 (external reference), with shifts downfield of the reference considered positive.

Synthesis of *mer*-Rh[$CH_2C(CH_3)_2(OH)$](PMe$_3$)$_3$(Cl)Br (4). To a solution of $Rh(PMe_3)_3Cl$ (143 mg, 0.390 mmol) in 7 mL of toluene at –30 °C was added a solution of 1-bromo-2-methyl-2-propanol (72.9 mg, 0.477 mmol) in 3 mL of toluene precooled to –30 °C. After 2 h at –30 °C, the solution was left at room temperature for 3 days. Needlelike crystals started forming after 1 day at room temperature. Filtration yielded 104 mg (52%) of a pale-yellow crystalline solid. Another portion of the complex can be obtained by concentration of the solvent. However, it is less pure and contaminated by another rhodium complex, probably an isomer of **4** in which the Cl/Br positions are exchanged. IR (Nujol): 3361 (s, sh), 1280 (m), 1276 (m), 1205 (m), 1119 (w), 945 (vs), 851 (w), 729 (s). ^1H NMR (toluene-d_8): δ 5.47 (br, s, 1H, OH), 1.52 (s, 6H, $2CH_3$), 1.42 (t, $^2J_{H-P}$ = 3.2 Hz, 18H, $2PMe_3$), 0.86 (d, $^2J_{H-P}$ = 9.4 Hz, 9H, $1PMe_3$). The signal for the CH_2Rh protons overlaps with the PMe_3 signal at 0.86 ppm. $^{31}P\{^1H\}$ NMR (THF): δ 11.7 (d of t, J_{P-Rh} = 133 Hz, $^2J_{P-P}$ = 35 Hz, 1P), –8 (d of d, J_{P-Rh} = 96 Hz, $^2J_{P-P}$ = 35 Hz, 1P). The other rhodium complex mentioned above in a mixture with **4** exhibits the following: $^{31}P\{^1H\}$ NMR (THF) δ 9 (d of t, $^2J_{P-P}$ = 35 Hz, 1P); J_{P-Rh} could not be measured exactly, –9.8 (d of d, $^2J_{P-Rh}$ = 95.7 Hz, $^2J_{P-P}$ = 34.9 Hz, 2P). $^{13}C\{^1H\}$ NMR (THF-d_8): δ 16.3 (t, J_{P-C} = 16 Hz, $2PMe_3$), 18.0 (d, J_{P-C} = 35 Hz, PMe_3), 33.8 (s, CH_3), 74.0 (s, CO) (Rh–CH_2 was not observed). Anal. Calcd: C, 30.04; H, 6.93; P, 17.91. Found: C, 29.73; H, 6.88; P, 17.52.

Synthesis of the Rhodaoxetane 5. Complex **4** (32 mg, 0.061 mmol) was suspended in 9 mL of toluene and cooled to –30 °C in a vial covered with aluminum foil. $(Me_3Si)_2NK$ (25 mg, 0.125 mmol) was suspended in 4 mL of toluene and the resulting suspension was filtered through cotton wool (approximately 20% was insoluble). The cloudy solution was cooled to –30 °C and added dropwise to the stirred solution of **4**. The reaction mixture became pale-yellow at the end of the addition. After 3 h at –30 °C, the solvent was evaporated to dryness to yield a brown oily residue which was extracted with C_6D_6 to yield the rhodaoxetane **5** (26 mg, 88%). IR (Nujol): 1298 (w), 1280 (vw), 1276 (m), 1213 (vw), 1138 (vw), 1055 (s), 1019 (m), 947 (vs), 879 (vw), 723 (m). ^1H NMR (benzene-d_6): δ 1.8–1.35 (br + 2s, 27H, PMe_3), 1.05 (m, 2H, CH_2–Rh), 0.88 (2s, 6H, CH_3). $^{31}P\{^1H\}$ NMR (benzene-d_6): δ –5 (d of t, $^2J_{P-Rh}$ = 118 Hz, $^2J_{P-P}$ = 35 Hz, 1P), –11 (d of d, $^2J_{P-Rh}$ = 104 Hz, $^2J_{P-P}$ = 35 Hz, 2P). $^{13}C\{^1H\}$ NMR (toluene-d_8): δ 6.2 (m, CH_2), 18.0 (d, J_{P-C} = 27 Hz, PMe_3), 34.7 (s, CH_3), 85.8 (t, $^2J_{C-Rh}$ = 7 Hz; $^3J_{C-P}$ = 7 Hz) (the triplet of the trans-disposed PMe_3 ligand is obscured by the solvent). Elemental analysis was not performed because of the small amounts of pure **5**. Crystals suitable for an X-ray structural study were grown by repeated freeze–thaw cycles of the C_6D_6 solution of **5**.

Reaction of 1-Bromo-2-methyl-2-propanol with Rh(PEt$_3$)$_3$Cl. Using conditions similar to those employed with $Rh(PMe_3)_3Cl$, only 35% conversion to a mixture of products was observed after 3 months at room temperature.

(28) Chatt, J.; Duncanson, L. A. *J. Chem. Soc.* **1953**, 2939.
(29) Ammeter, J. H.; Bürgi, H.-B.; Thibeault, T. C.; Hoffmann, R. *J. Am. Chem. Soc.* **1978**, *100*, 3686.
(30) Mealli, C.; Proserpio, D. M. *J. Chem. Educ.* **1990**, *66*, 399.

Reaction of 1-Chloro-2-methyl-2-propanol with Rh(PMe_3)$_3$Cl. No reaction was observed under conditions similar to those employed with 1-bromo-2-methyl-2-propanol. Heating at 65 °C for 5 h led to the formation of a mixture which does not include the expected oxidative addition product.

Reaction of Rh(PMe_3)$_3$Br with Isobutylene Oxide. To a solution of 150 mg of Rh(PMe_3)$_3$Br in 2 mL of THF under nitrogen was added dropwise 0.5 mL of isobutylene oxide. The solution was stirred at room temperature, resulting in decoloration. The solvent and excess epoxide were removed under high vacuum, and the residue was dissolved in C_6D_6. $^{31}P\{^1H\}$ NMR analysis revealed that the mixture contained approximately 30% of the metallaoxetane **5**, in addition to other unidentified complexes.

1-Bromo-2-methyl-2-propanol (2). This compound was prepared according to a general literature procedure for bromohydrine synthesis[31] from isobutylene and *N*-bromosuccinimide in 55% yield. Bp: 56–8 °C (30 mmHg), lit.[32] 62.5–66 °C (31 mmHg). ^1H NMR ($CDCl_3$): δ 3.45 (br, s, 2H, CH_2–Br), 2.18 (br, s, 1H, OH), 1.35 (br, s, 6H, CH_3).

Crystal Structure Determinations of 4 and 5. Single crystals of **4** and **5** were obtained as described above. The crystal was mounted on the diffractometer equipped with a low temperature device. Summaries of the data collection parameters are given in Table I. Data were corrected for Lorentz, polarization, and absorption effects. The structures were solved by automated Patterson analysis (SHELX-86) and Fourier methods (SHELX-76). The hydrogen atoms were found from the difference Fourier map and refined. The illustrations were drawn with ORTEP-II.[33] A list of bond distances and angles is given in Tables II and III. All details are given in the supplementary material.

Acknowledgment. This work was partially supported by Junta Nacional de Investigação Científica e Tecnológica (PMCT/C/CEN/367/90 and Grant BD/BIC/169/90/RM to A.M.G.). Financial support by the U.S.-Israel Binational Science Foundation (BSF), Jerusalem, Israel (Grant No. 89-00374 to D.M.) is gratefully acknowledged. D.M., A.A.Z., and F.F. thank Prof. J. P. Collman (Stanford University) for helpful discussions and for his interest in this work. C.Ü. thanks the Turkish Scientific and Research Council (TUBITAK).

Supplementary Material Available: Textual presentation of crystal data, tables of atom coordinates, anisotropic temperature factors, hydrogen atom coordinates, bond lengths, bond angles, and torsion angles, and packing diagrams for **4** and **5** (14 pages). Ordering information is given on any current masthead page.

OM9302305

(31) Guss, C. O.; Rosenthal, R. *J. Am. Chem. Soc.* **1955**, *77*, 2549.
(32) Traynham, J. G.; Pascual, O. S. *Tetrahedron* **1959**, *7*, 165.
(33) Johnson, C. K. ORTEP-II. Report ORNL-5138; Oak Ridge National Laboratory: Park Ridge, TN, 1976.